Fractal dimension algorithms and their application to time series associated with natural phenomena

F Cervantes-De la Torre[1], J I González-Trejo[1], C A Real-Ramírez[1] and L F Hoyos-Reyes[1]

[1] Departamento de Sistemas, División de Ciencias Básicas e Ingeniería, Universidad Autónoma Metropolitana-Azcapotzalco, Av. San Pablo 180, Col. Reynosa Tamaulipas, Delegación Azcapotzalco, C.P. 02200, México. D. F., México

E-mail: fcdt@correo.azc.uam.mx

Abstract. Chaotic invariants like the fractal dimensions are used to characterize non-linear time series. The fractal dimension is an important characteristic of systems, because it contains information about their geometrical structure at multiple scales. In this work, three algorithms are applied to non-linear time series: spectral analysis, rescaled range analysis and Higuchi's algorithm. The analyzed time series are associated with natural phenomena. The disturbance storm time (Dst) is a global indicator of the state of the Earth's geomagnetic activity. The time series used in this work show a self-similar behavior, which depends on the time scale of measurements. It is also observed that fractal dimensions, D, calculated with Higuchi's method may not be constant over-all time scales. This work shows that during 2001, D reaches its lowest values in March and November. The possibility that D recovers a change pattern arising from self-organized critical phenomena is also discussed.

1. Introduction

Solar storms consist of three major components: solar flares, solar proton events and coronal mass ejections (CMEs). Not all solar storms produce all of these elements, but the largest solar storms tend to do it. CMEs can interact with Earth's magnetic field to produce a geomagnetic storm, this produce a temporary disturbance of the Earth's magnetosphere and an equatorial ring of currents, differential gradient and curvature drift of electrons and protons in the near Earth region [12].

There is a global index, the disturbance storm time (Dst), which was devised as a mean for characterizing the level of disturbance observed in the equatorial regions. As it has been long observed, the north-south horizontal component of the geomagnetic field becomes depressed during major geomagnetic storms, and this is more pronounced in equatorial and low-latitude regions. Several studies proved that the degree and extent of this depression are useful tools for characterizing the energy transfer from solar wind into the Earth's magnetosphere. They also provide an estimate of the energy density of the energetic particles in the Earth's ring currents.

The Dst index is computed once per hour, and their measurements are usually expressed in nano-Tesla (nT). The Dst index has negative values. A severe geomagnetic storm is defined as any event with a Dst value lower than $-500nT$. An estimated Dst value for the "1859 Carrington event" (described later in the paper) was $-1760nT$ [8]. The storm responsible for the Quebec

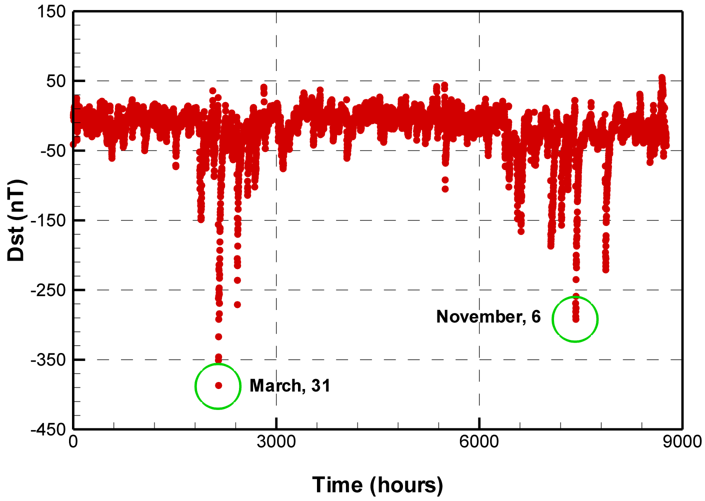

Figure 1. Dst time series for 2001. The intense magnetic storms occurred on March 31st and the November 6th, with minimum Dst values of $-387nT$ and $-292nT$ respectively.

power outage, which occurred in 1989 (also described later in this work), registered a Dst value of $-589nT$.

There are several space weather phenomena associated with geomagnetic storms [12]: (i) shifting of the Van Allen radiation belt and geomagnetically induced currents (GICs), which can flow through power transmission grids (as well as pipelines and undersea cables) and lead to power system problems, (ii) ionospheric disturbances which cause radio and radar scintillation, (iii) disruption of navigation by magnetic compass, and (iv) auroral boreal displayed at much lower latitudes than normal.

Solar storms vary in size and impact on Earth. One of the largest solar storms occurred in September of 1859 (Dst = -1,760 nT). This particular solar storm is known as the "Carrington flare". In 1989, from August 28th to September 4th, auroral displays, often called as northern or southern lights, spanned on several continents and were observed around the world. A British amateur astronomer, Richard Carrington, recorded the solar outburst, a white-light flare. According to modern experts, the "Carrington flare" were actually two intense geomagnetic storms. Across the world, telegraph networks experienced disruptions and outages as a result of the currents generated by the geomagnetic storms. The economic costs associated with a catastrophic event similar to the Carrington flare could reach several trillion dollars [11].

On March 13th, 1989, a geomagnetic super-storm ($Dst = -589nT$) affected Canadian and U.S. power systems, resulting in a major power outage for nine hours for the majority of the Quebec region and the northeastern of United States. The Hydro-Quebec grid's geographic location and its 1,000 km transmission lines made it susceptible to geomagnetic storm. Central and southern Sweden also experienced power losses when GICs disrupted six $130kV$ power lines. The GICs flowed through the power system, causing severe damages to seven static compensators on the La Grande network in the Hydro-Quebec grid. The loss of the compensators resulted in a system disturbance and severe equipment damage. After nine hours, 83 percent of the total power was restored, but a million customers remained without electric power. The total cost of the Hydro-Quebec incidents is estimated to be $6 billion. Since the incident, the Canadian government has set up protective measures at the Hydro-Quebec sit e, such as transmission-line series capacitors, whose cost was more than $1.2 billion, which prevent the system from being damaged again by the GICs.

Because our civilization has evolved into a technology dependent society, today a solar storm of this magnitude or greater could produce a global catastrophe.

2. Scaling law and invariants quantities

This section presents a brief discussion about certain quantities, invariant under smooth coordinate transformations. The theory of nonlinear dynamical systems provides new tools and quantities for the characterization of irregular time-series data through universal scaling laws, such as the spectral analysis, rescaled range analysis and Higuchi's algorithm.

2.1. Spectral exponent β

The time evolution of a dynamic system is represented by the time variation $X(t)$ or (when sampled at regular intervals) time series of its dynamic variables. Any function $X(t)$ may be usually represented as the superposition of periodic components. The determination of their relative strengths is called spectral analysis.

If a time series $X(t)$ is specified over a time interval T, the mean signal $\bar{X}(t)$ is given by

$$\bar{X}(t) = \frac{1}{T}\int_0^1 X(t)dt \tag{1}$$

The variance σ^2, of the signal $X(t)$, is defined by

$$\sigma^2(X(t)) = \mathrm{Var}(X(t)) = \frac{1}{T}\int_0^1 [X(t) - \bar{X}(t)]^2 dt \tag{2}$$

and the standard deviation σ is the square root of the variance.

The mean and the variance are the first two moments of the time series. The time series $X(t)$ can be represented in the frequency domain f, in terms of the amplitude $A(f,T)$, which is the Fourier transform of $X(t)$:

$$A(f,T) = \int_{-\infty}^{\infty} X(t)e^{2\pi i f t}dt \tag{3}$$

The inverse Fourier transform is

$$X(t) = \int_{-\infty}^{\infty} A(f,T)e^{-2\pi i f t}df \tag{4}$$

The quantity $\mid A(f,T) \mid^2$ is the contribution to the total energy of $X(t)$ from components with frequencies in $[f, f+df]$. In real time series, the samples are picked up in a finite interval $0 < t < T$, in such a way that the effect of finite time series shall be taken into account. The FFT method (Fast Fourier Transform) is the appropriate tool to analyze this kind of systems [3]. The power spectral density of $X(t)$ is defined by:

$$s(f) = \lim_{T\to\infty} \frac{1}{T} \mid A(f,T) \mid^2 \tag{5}$$

The quantity $s(f)df$ is the power in the time series associated with the frequency in the interval $[f, f+df]$. If a time series is fractal, then it satisfies the following power law relation:

$$s(f) \propto f^{-\beta} \tag{6}$$

Where β is a constant that defines the kind of dynamic behavior of the time series $X(t)$. For example, $\beta = 0$ for white noise-like systems, which are uncorrelated and have a power spectrum that is independent of the frequency. Another relevant case is $\beta = 1$, the so-called flicker or $1/f$ noise systems, which are moderately correlated. For Brownian noise-like systems, $\beta = 2$, which are strongly correlated.

2.2. Hurst exponent H

The Hurst exponent is commonly used as a measure of the geometric fractal scaling in a data series [10]. If the series $X(t)$ is a self-affine fractal, then $X(bt)$ is statistically equivalent to $b^H X(t)$, where H is the Hurst exponent. Many methods for estimating Hurst's exponent have been proposed and used in the literature. Each of these methods has specific advantages and disadvantages. In our research, we focus on classical methods of rescaled range analysis [7].

The rescaled range R/S statistics for discrete time series (X_t) is defined as follows:

$$Y(t,\tau) = \sum_{i=0}^{t-1} [X_i - \langle X \rangle_\tau] \tag{7}$$

$$R(\tau) = \max_{0\le t\le \tau-1} Y(t,\tau) - \min_{0\le t\le \tau-1} Y(t,\tau) \tag{8}$$

$$S(\tau) = \left(\frac{1}{\tau} \sum_{t=0}^{\tau-1} (X_t - \langle X \rangle_\tau)^2 \right)^{\frac{1}{2}} \tag{9}$$

$$R/S(\tau) = \frac{R(\tau)}{S(\tau)} \tag{10}$$

We can now apply

$$\frac{R}{S} \propto \tau^H \tag{11}$$

The values of the Hurst exponent vary between 0 and 1. A Hurst exponent value of $H = 0.5$ indicates a random walk process (a Brownian motion). In a random walk, there is no correlation, this is uncorrelated time series. If $0 \le H \le 0.5$, the process is said to be antipersistent. The system is covering smaller distances than a random walk process. This means that an increase will tend to be followed by decrease (or decrease will be followed by an increase). This behavior is sometimes called mean reversion. For $0.5 < H \le 1$, the time series belongs to a persistent process. This series covers more distance than a random walk process. Thus, if the system increases in one period, it is more likely to keep increasing in the next period.

2.3. Higuchi's algorithm

In this section, we briefly discuss the Higuchi's algorithm. This is a technique for calculating the fractal dimension D, of a time series. The power spectrum analysis has been used as a useful and efficient method to analyze irregular time series, especially if the Power Spectrum follows the Power Law (6). The exponent β in (6) is considered to be the index (invariant) for representing the irregularity of a time series. We have demonstrated in [5] that in many cases, the usage of the Higuchi's fractal dimension D, is more appropriate than the spectral exponent β.

In order to obtain the fractal dimension D, Higuchi [6] considered a finite set of observations, taken at a regular interval:

$$X(1),\ X(2),\ X(3),\ \ldots,\ X(N). \tag{12}$$

From this series, a new one X_k^m, must be constructed, which is defined as follows:

$$X_k^m;\ X(m),\ X(m+k),\ X(m+2k),\ldots,\ X\left(m + \left[\frac{N-m}{k}\right] k\right), \tag{13}$$

with $(m = 1, 2, \ldots, k)$; and where $[\cdot]$ denotes the Gauss notation, that is the bigger integer, and both k and m are integers. m and k indicate the initial time and the interval time, respectively.

For a time interval equal to k, one gets k sets of new time series. For example, for $k = 4$ and $N = 100$, four new time series are obtained

$$\begin{array}{r} X_4^1 : \; X(1), \, X(5), \, X(9), \, \ldots, \, X(97) \\ X_4^2 : \; X(2), \, X(6), \, X(10), \, \ldots, \, X(98) \\ X_4^3 : \; X(3), \, X(7), \, X(11), \, \ldots, \, X(99) \\ X_4^4 : \; X(4), \, X(8), \, X(12), \, \ldots, \, X(100) \end{array} \tag{14}$$

Higuchi [6], defines the length of the curve associated to each time series, X_k^m as follows:

$$L_m(k) = \frac{1}{k}\left(\sum_{i=1}^{\left[\frac{N-m}{k}\right]} \left(X(m+ik) - X(m+(i-1)k)\right)\right)\left(\frac{N-1}{\left[\frac{N-m}{k}\right]k}\right) \tag{15}$$

where the term

$$\frac{N-1}{\left[\frac{N-m}{k}\right]k}, \tag{16}$$

represents a normalization factor. Higuchi takes the average value $\langle L(k)\rangle$ of the lengths associated to the time series given by Equation (15).

If the average value follows a power law:

$$\langle L(k)\rangle \propto k^{-D}, \tag{17}$$

then the curve is fractal with dimension D. Higuchi's algorithm can be applied even over time series that are not stationary. This fact represents an advantage over spectral analysis [5] and Hurst's algorithm.

The spectral exponent β is related with the fractal dimension D of the time series, and with exponent H, know as the Hausdorff measure, by means of the following relation [4, 10]:

$$\beta = 2H + 1 = 5 - 2D \tag{18}$$

Higuchi [6] showed that if $1 \leq \beta \leq 3$, then $D = (5 - \beta)/2$. He also shows that the following limits are held:

$$\text{if } \beta \to 0 \text{ then } D \to 2 \tag{19}$$

which corresponds to uncorrelated white noise. The second limit is:

$$\text{if } \beta \to 3 \text{ then } D \to 1 \tag{20}$$

Since the values of the fractal dimension D for Dst index time series are in the interval $[1, 2]$, equations (18), (19) and (20) can be used for analyzing it.

3. Time evolution of the index Dst

We study the evolution of the Dst index along the 2001 year. In this year, two intense magnetic storms were registered. One of them occurred on March 31st, and the other one was on November 6th (see Figure 1). The minimum Dst values were $-387nT$ and $-292nT$, respectively.

Through the power laws (6), (11) and (17), we calculated the fractals exponents β, H and D.

The analysis of data belonging the months of March, April and November, is shown in Figures 2, 4 and 6, respectively. The upper panel on each of these figures shows the time evolution of

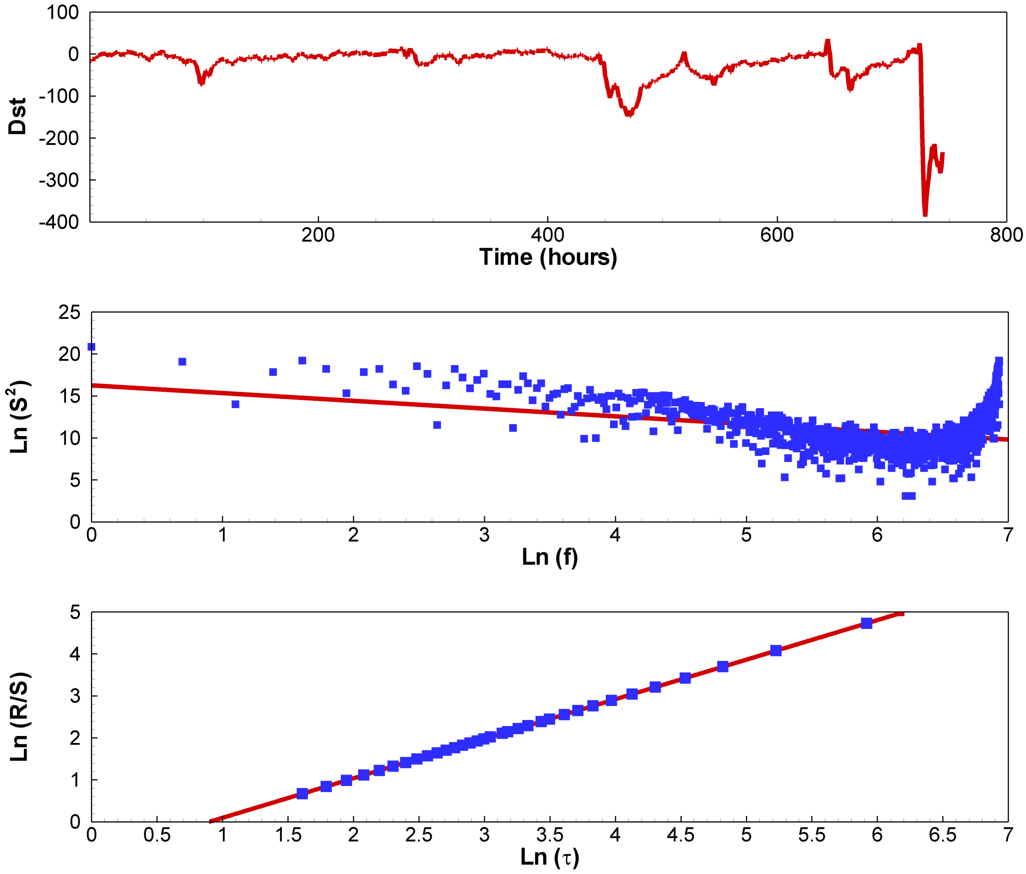

Figure 2. Analysis of data for March month. Dst time series (upper panel). Power laws of the spectral analysis (middle panel). Rescaled range analysis (bottom panel).

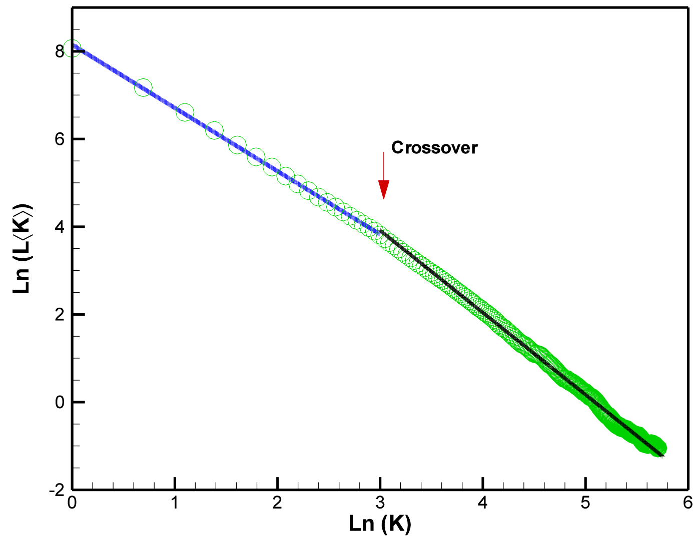

Figure 3. Analysis of data for March month trough Higuchi's algorithm.

the Dst index. The middle panel displays the results of the spectral analysis. The bottom panel shows the rescaled range and the Hurst's algorithm analysis for the corresponding month. The analysis of the Dst index time series through Higuchi's algorithm for the months of March, April

Journal of Physics: Conference Series **475** (2013) 012002 doi:10.1088/1742-6596/475/1/012002

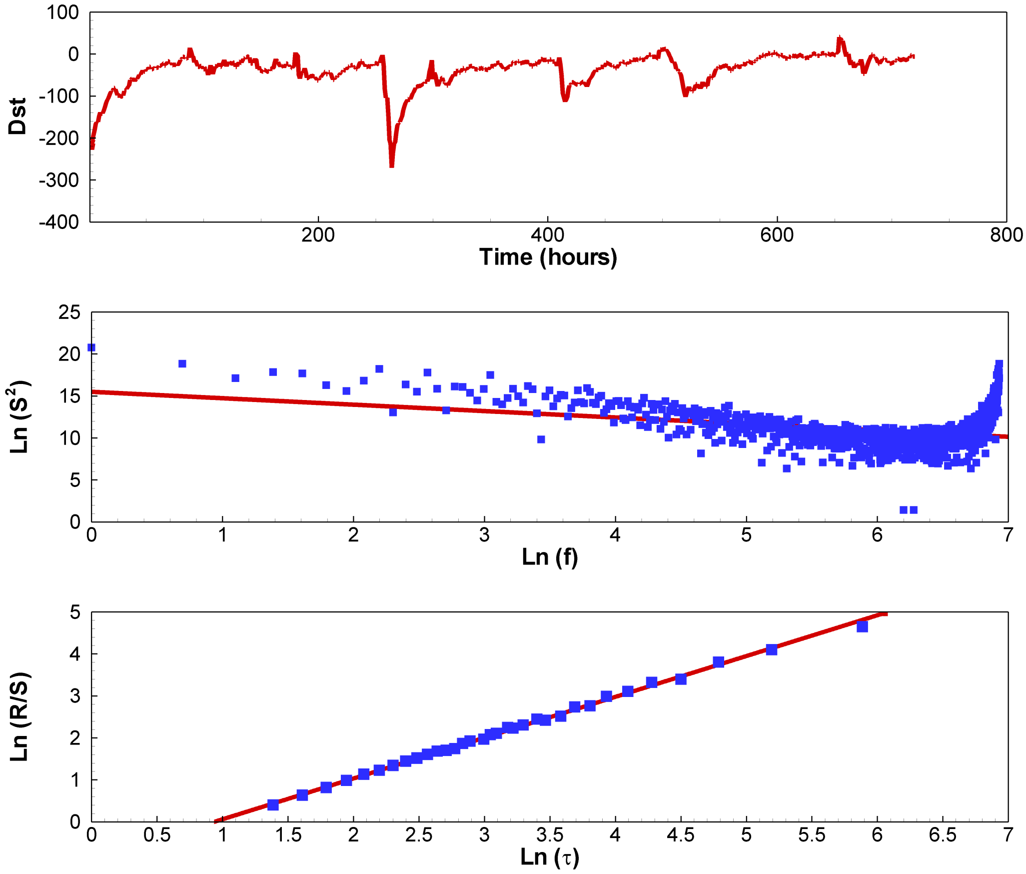

Figure 4. Analysis of data for April month. Dst time series (upper panel). Power laws of the spectral analysis (middle panel). Rescaled range analysis (bottom panel).

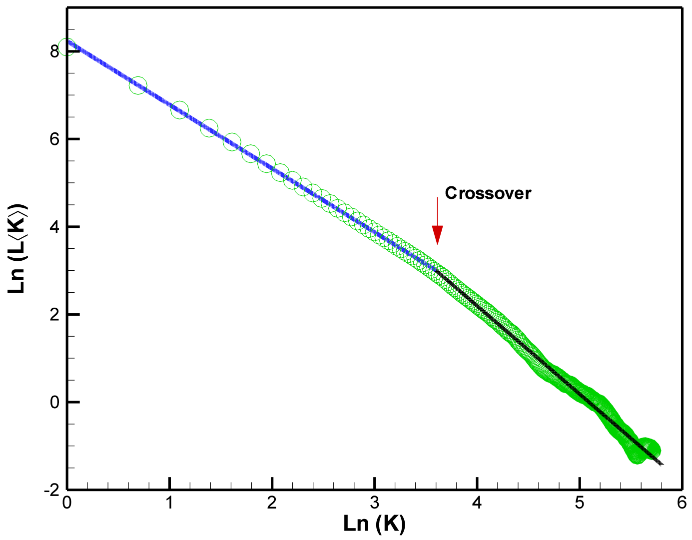

Figure 5. Analysis of data for April month trough Higuchi's algorithm.

and November, is shown in Figures 3, 5 and 7, respectively.

The best least-squares fit for the spectral analysis are reported in Table 1.

The values of the correlation coefficient show very poor results. In Figures 2, 4 and 6, the

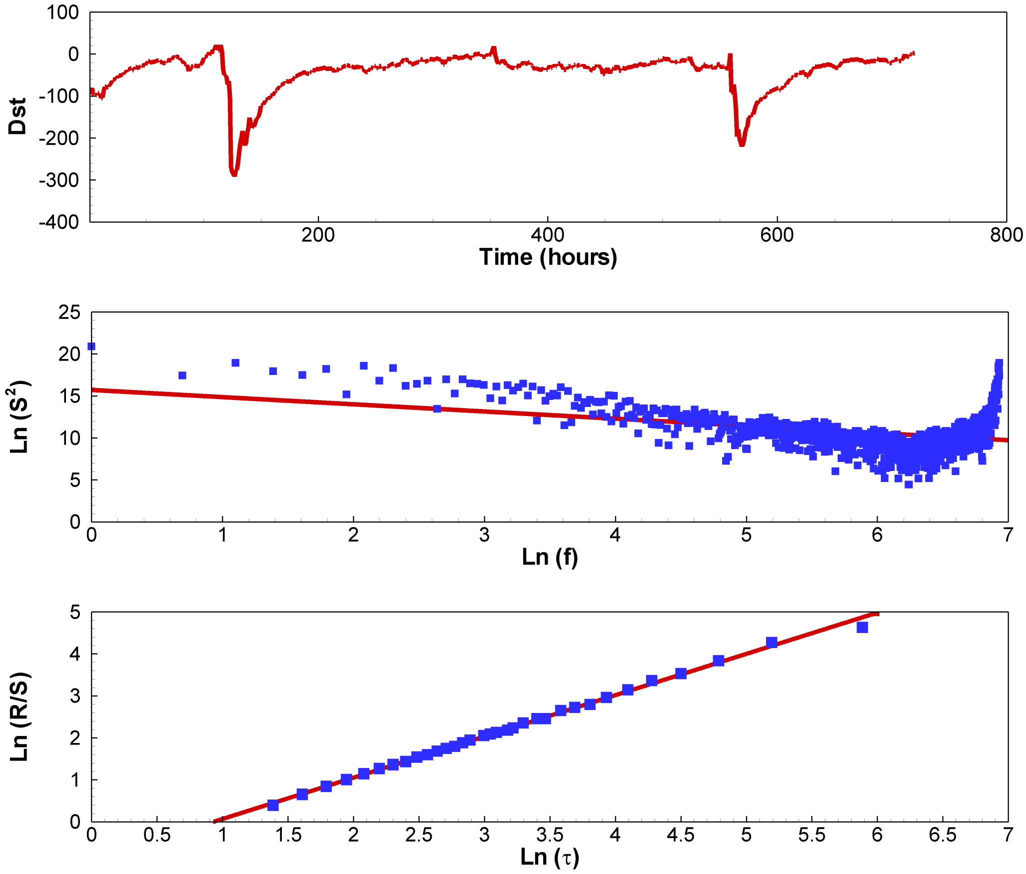

Figure 6. Analysis of data for November month. Dst time series (upper panel). Power laws of the spectral analysis (middle panel). Rescaled range analysis (bottom panel).

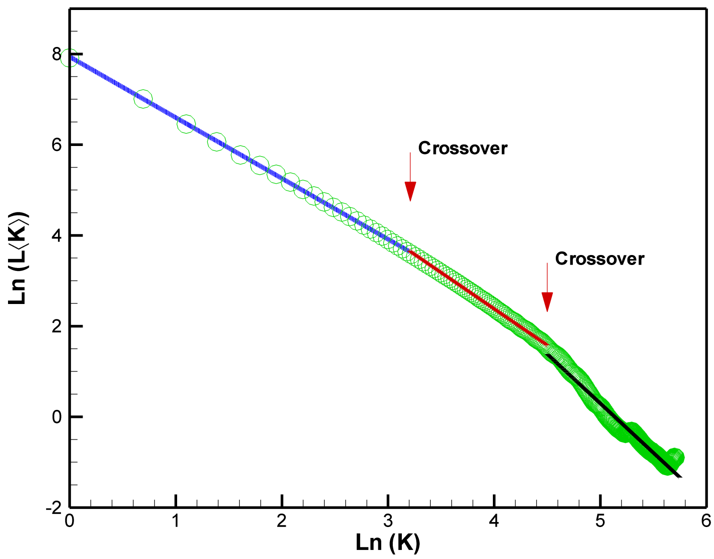

Figure 7. Analysis of data for November month trough Higuchi's algorithm.

power spectra obtained by the FFT-method show noisy fluctuations superposed on the power law spectrum. Thus, the unambiguous determination of the exponent β is difficult.

Table 1. Spectral Analysis

Month	Fractal exponent	
March	$\beta = 0.9221 \pm 0.07666$	$R^2 = 0.1232$
April	$\beta = 0.7648 \pm 0.06314$	$R^2 = 0.1247$
November	$\beta = 0.8552 \pm 0.06858$	$R^2 = 0.1312$

Table 2. Rescaled range analysis

Month	Fractal exponent	
March	H $= 0.9417 \pm 0.004806$	$R^2 = 0.9981$
April	H $= 0.9718 \pm 0.004336$	$R^2 = 0.9985$
November	H $= 0.9828 \pm 0.004573$	$R^2 = 0.9984$

Table 3. Higuchi's algorithm

Month	Fractal exponent	
March	D1 $= 1.4693 \pm 0.009344$	$R^2 = 0.99891$
	D2 $= 1.8843 \pm 0.005491$	$R^2 = 0.99770$
April	D1 $= 1.4395 \pm 0.007237$	$R^2 = 0.99937$
	D2 $= 1.9975 \pm 0.009496$	$R^2 = 0.99387$
	D1 $= 1.3558 \pm 0.005275$	$R^2 = 0.99953$
November	D2 $= 1.6284 \pm 0.005694$	$R^2 = 0.99933$
	D3 $= 2.0189 \pm 0.023000$	$R^2 = 0.97719$

The best least-squares fit for the rescaled range and the Hurst's algorithm are reported in Table 2.

The results of the Higuchi's algorithm applied to Dst time series for the months of March, April and November are reported in Table 3.

Although the statistical results of the rescaled range analysis are good, Higuchi's algorithm apparently contains more information about the dynamics of the time series. We found that when Higuchi's algorithm is applied to Dst index time series, a crossover behavior is revealed. For March and April months, we found that $\langle L(k) \rangle$ exhibits a crossover between two distinct fractal dimension D. The analysis applied to November data revealed three values for D.

Several values of D are contained in the interval $(1.3, 1.7)$, whereas there are other values of$D$ too close to 2, which correspond to a uncorrelated, white noise like signal. Changes in the fractal dimension D can be associated with changes in the dynamics of the Dst index time series.

The D values of Dst for 2001 year between 1.3 and 1.7, corresponds to values of the spectral exponent β, between 1.6 and 2.4; that is, some values in the range of Fractional Brownian

Motion [10]. If β is in the interval $(1.6, 2.4)$, then the exponent H, is in the interval $(0.3, 0.7)$ (see equation 2), indicating that some process has long range autocorrelations or antipersistence [9]. That is, the signal has a behavior such that an increasing trend in the past implies a decreasing trend in the future and vice versa. For Brownian noise, $H = 0.5$, $D = 1.5$ and $\beta = 2$. These results agree with those obtained by Balasis *et al.* [2].

4. Concluding remarks

In this work, we compared three analysis techniques, the spectral exponent β, calculated by means of the FFT algorithm, the Hurst exponent H, calculated by rescaled range analysis, and the fractal dimension D, calculated by using the Higuchi's algorithm.

We show that the FFT-methods leads to very poor correlation coefficients. Despite the Hurst exponent H has good statistical properties, the existence of different dynamics in the time series is not shown in detail.

On the other hand, the usage of the Higuchi's method leads to very precise values of the fractal dimension D, associated with the Dst time series. This algorithm also shows the complexity (crossover existence) of the time series studied.

For the case studied in this work, we found that D corresponds to representative values of Fractional Brownian noise. A possible explanation of these results is related with the concept of self-organized criticality (SOC) [1]. The SOC concept was developed for complex systems, which are reminiscent of typical geological structures. The notion of SOC was proposed by Bak *et al.* [1] as a general principle governing the behavior of a spatially extended dynamical system with both, temporal and spatial degree of freedom. According to this principle, composite open systems having many interacting elements organize themselves into a stationary critical state with no length or time scales others than those imposed by the finite size of the system. The critical state is characterized by spatial and temporal power laws.

Acknowledgments

The Dst data were provided by the World Data Center for Geomagnetism, Kyoto. (http://swdcwww.kugi.kyoto-u.ac.jp)

Authors acknowledge the financial support from Sistema Nacional de Investigadores (SNI - CONACYT). The data numerical analysis was done at the Laboratorio de Computo Cientifico, Departamento de Sistemas, at Universidad Autonoma Metropolitana - Azcapotzalco.

References

[1] Bak P and Tang C 1989 Earthquake as a self-organized critical phenomenon *J. Geophys. Res.* **54** 15635-37
[2] Balasis G, Ioannis A D, Anastasios A and Konstantinos E 2008 Detection of dynamical complexity changes in Dst time series using entropy concepts and rescaled range analysis *Geophys. Res. Let.* **35** L14102
[3] Birgham E O 1988 *The fast Fourier transform and its applications* (New Jersey: Prentice Hall)
[4] Burlaga L F and Klein L W 1986 Fractal structure of the interplanetary magnetic field. *J. Geophys. Res.* **91A1** 347-350
[5] Cervantes-De la Torre F, Ramírez-Rojas A, Pavía-Miller C G, Angulo-Brown F, Yépez E and Peralta J A 1999 A comparison between spectral and fractal methods in electrotelluric time series *Rev. Mex. Fis.* **45** 298-302
[6] Higuchi T 1988 Approach to an irregular time series on basis of the fractal theory *Physica* D **31** 277-283
[7] Hurst H E 1951 Long term storage capacity of reservoirs *Trans. Am. Soc. Civ. Eng.* **116** 770-779
[8] Lankhina G S, Alex S, Tsurutani B T, and Gonzalez W D 2004 Research on historical records of geomagnetic storms *Proc. of the Int. Astronomical Union* vol. 2004 issue IAUS226 (Cambridge University Press) pp 3-15
[9] Rangarajan G and Ding M 2000 Integrated approach to assessment of long range correlation in time series data. *Phys. Rev.* E **61** 4991-5001
[10] Turcotte D L 1992 *Fractals and chaos in geology and Geophysics* (Cambridge University Press)
[11] U.S. House Homeland Security Committee, 2009 http://www.dhs.gov/files/programs/gc_1225921753386.shtm
[12] Wikipedia http://en.wikipedia.org/wiki/Solar_storm